frontiers in Materials

ORIGINAL RESEARCH
published: 08 February 2022
doi: 10.3389/fmats.2022.832703

Investigations on Strong-Tuned Magnetocaloric Effect in $La_{0.5}Ca_{0.1}Ag_{0.4}MnO_3$

Mahmoud A. Hamad[1] and Hatem R. Alamri[2]*

[1]Basic Science Department, Higher Institute of Engineering and Technology, King Marriott Academy, Alexandria, Egypt, [2]Physics Department, Aljamoum-University-College, Umm Al-Qura University, Makkah, Saudi Arabia

The magnetocaloric effect (MCE) of $La_{0.5}Ca_{0.1}Ag_{0.4}MnO_3$ (LCAMO) is simulated using a phenomenological model (PM). The LCAMO MCE parameters are calculated as the results of simulations for magnetization *vs*. temperature at different values of external magnetic field (H_{ext}). The temperature range of MCE in LCAMO grew as the variation in H_{ext} increased, eventually covering the room temperature at high H_{ext} values. The MCE of LCAMO is tunable with the variation of H_{ext}, proving that LCAMO is practically more helpful as a magnetocaloric (MC) material for the development of magnetic refrigerators in an extensive temperature range, including room temperature and lower and higher ones. The MCE parameters of LCAMO are practically greater than those of some MC samples in earlier works.

Keywords: magnetocaloric effect, phenomenological model, phase transition, perovskite, entropy change

OPEN ACCESS

Edited by:
Wissem Cheikhrouhou-Koubaa, Centre de Recherche en Numérique de Sfax (CRNS), Tunisia

Reviewed by:
Rachid Masrour, Sidi Mohamed Ben Abdellah University, Morocco
Gaofeng Wang, Inner Mongolia University of Science and Technology, China

****Correspondence:***
Mahmoud A. Hamad
m_hamad76@yahoo.com

Specialty section:
This article was submitted to Semiconducting Materials and Devices, a section of the journal Frontiers in Materials

Received: *10 December 2021*
Accepted: *04 January 2022*
Published: *08 February 2022*

Citation:
Hamad MA and Alamri HR (2022) Investigations on Strong-Tuned Magnetocaloric Effect in $La_{0.5}Ca_{0.1}Ag_{0.4}MnO_3$. Front. Mater. 9:832703. doi: 10.3389/fmats.2022.832703

INTRODUCTION

The need to solve the problem of emission of hazard gases, which come out of conventional vapor refrigerators, results in increased interest in functioning magnetic refrigerator (MR), the idea of which depends on functioning magnetocaloric effect (MCE) (Dhahri et al., 2014; El-Sayed and Hamad, 2019a; El-Sayed and Hamad, 2019b; Ahmed et al., 2021a, Ahmed et al., 2021b; Hamad et al., 2021; Jebari et al., 2021), because the MR provides high efficiency for cooling without any negative impact on the environment and has low energy consumption, availability of mechanical stability, and fewer noise events during cooling operation (Dhahri et al., 2015; Hamad, 2015a; ErchidiElyacoubi et al., 2018a, ErchidiElyacoubi et al., 2018b; Hamad et al., 2020; Sharma et al., 2020; Belhamra et al., 2021). MCE is described as a change in magnetic entropy (ΔS_M) with a variation in the external magnetic field (H_{ext}) exerted on the material, causing a change in temperature (Masrour et al., 2016; ErchidiElyacoubi et al., 2018c; Kadim et al., 2020, Kadim et al., 2021a, Kadim et al., 2021b). Numerous research over decades have studied various magnetic materials to discover their suitability as magnetocaloric (MC) materials suitable for the MR industry (Hamad, 2015b; Masrour et al., 2017; Jebari et al., 2021; Labidi et al., 2021). It is preferable to use MC materials that have a magnetic transition type of the second degree with a suitable Curie temperature (θ_C) as appropriate for use in a wide temperature range, including room temperature (Choura-Maatar et al., 2020; Henchiri et al., 2020; Laajimi et al., 2020). The current efforts are directed towards the use of manganite as an effective substance in MRs due to its great chemical stability during frequent use, lack of eddy current, ease of preparation, high electrical resistance, and the possibility of improving their properties through doping and changing the oxygen content (Alzahrani et al., 2020; Choura-Maatar et al., 2020; Henchiri et al., 2020; Laajimi et al., 2020). Felhi *et al.* prepared

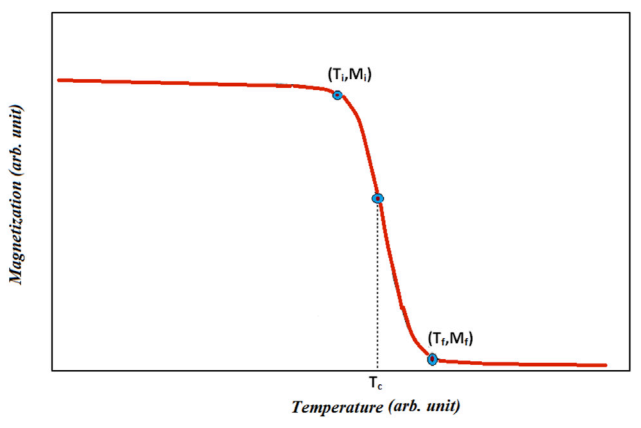

FIGURE 1 | Isofield magnetization *vs*. temperature.

$La_{0.5}Ca_{0.1}Ag_{0.4}MnO_3$ (LCAMO) *via* the ceramic method and reported an increase in H_{ext} and an increase in broad ferromagnetic (FM) phase transition of LCAMO covering room temperature under high H_{ext} (Jeddi et al., 2020). These results motivate us to investigate the MCE of LCAMO, expecting that the MCE of LCAMO covers a large range of temperatures, especially cryogenic temperature and room temperature. Furthermore, it is believed that LCAMO, as a manganite, has low material processing costs, high chemical stability, and high resistivity, which are advantageous for reducing the overall eddy current heating. In this research, the MCE of LCAMO is studied using a phenomenological model (PM) to simulate the isofield magnetization *vs*. temperature curves, concluding with simulated ΔS_M, heat capacity change ($\Delta C_{P,H}$), and relative cooling power (RCP).

THEORETICAL CONSIDERATIONS

According to PM, as described in Hamad (2012, 2015c, 2015d), the magnetization (M) *vs*. temperature is simulated by:

$$M(T) = \left(\frac{M_i - M_f}{2}\right)[\tanh(\alpha(\theta_C - T))] + \beta(T - \theta_C) + \left(\frac{M_i + M_f}{2}\right) \quad (1)$$

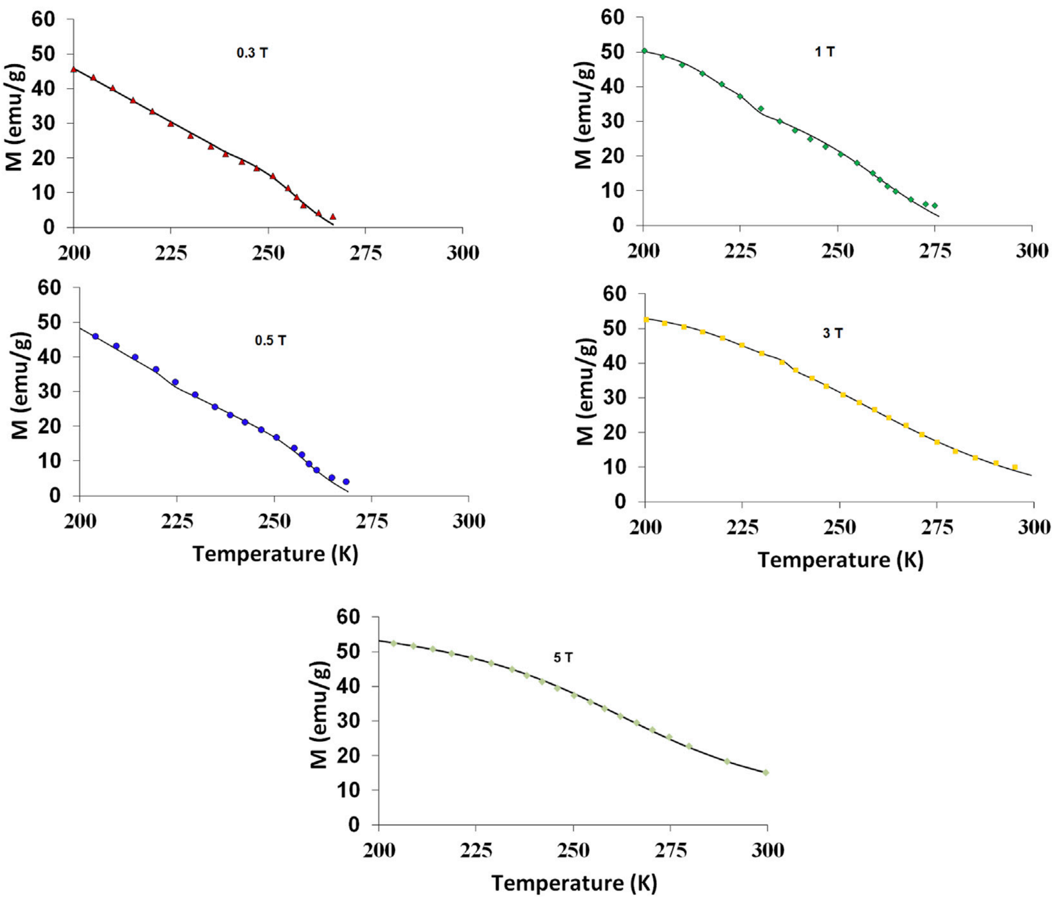

FIGURE 2 | Magnetization *vs*. temperature for $La_{0.5}Ca_{0.1}Ag_{0.4}MnO_3$. The dashed curves are modeled results, and the symbols represent experimental data from Jeddi *et al*. (2020).

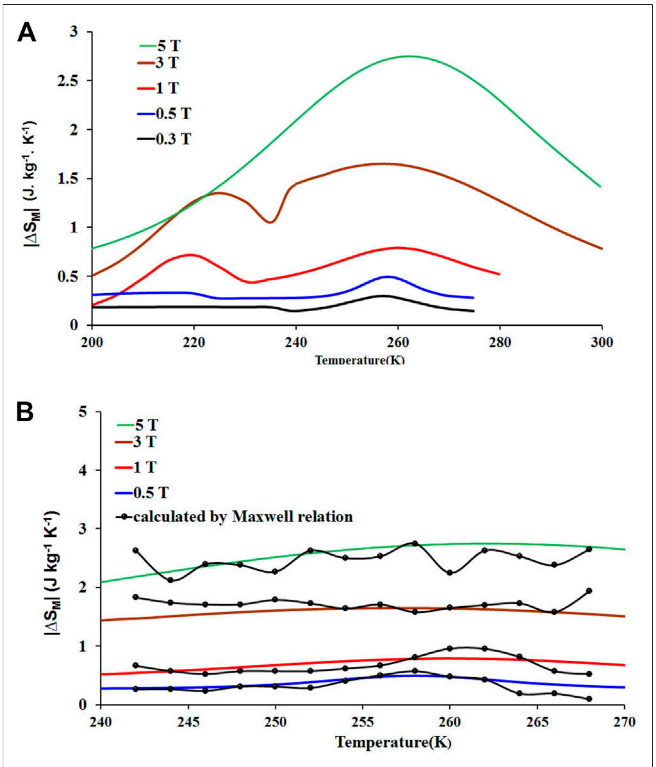

FIGURE 3 | (A) ΔS_M and **(B)** $\Delta S_M(T)$ was calculated by Maxwell relation, and $\Delta S_M(T)$ was calculated by a phenomenological model.

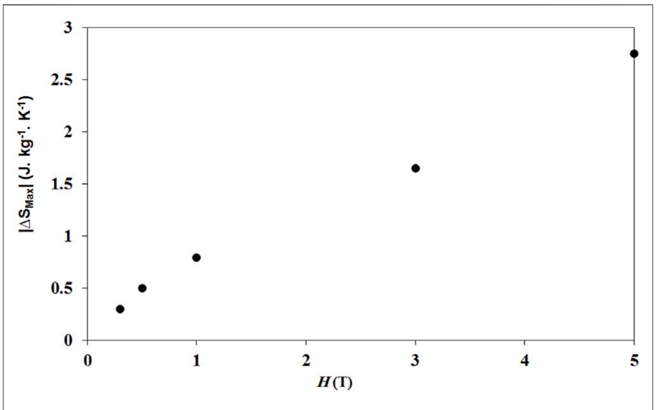

FIGURE 5 | $|\Delta S_{Max}|$ *vs.* ΔH for $La_{0.5}Ca_{0.1}Ag_{0.4}MnO_3$.

where M_i and M_f are values of magnetization at the onset and finalization of the FM paramagnetic transition as pointed out in **Figure 1**, respectively.

$$\alpha = \frac{2(\beta - \gamma)}{M_i - M_f} \tag{2}$$

where $\gamma = (\frac{dM}{dT})_{T=\theta_C}$.

$$\beta = \left(\frac{dM}{dT}\right)_{average} \text{ for FM phase} \tag{3}$$

The numerical evaluation of ΔS_M of LCAMO under H_{ext} variation (ΔH) can be derived from Maxwell's relation and derived from **Eq. 1** as follows:

$$\Delta S_M = \int_0^{H_{max}} \left(\frac{\partial M}{\partial T}\right)_H dH = \left(-(\beta - \gamma)\,\mathrm{sech}^2(\alpha(\theta_C - T)) + \beta\right)\Delta H. \tag{4}$$

From **Eq. 4**, we can easily calculate $\Delta S_M(T)$ by determining the M_i, M_f, θ_c, β, and γ from isofield $M(T)$ curves. Moreover, a maximum value of $\Delta S_M(\Delta S_{Max})$, where $T = \theta_C$, can be assessed according to the following equation:

$$\Delta S_{Max} = \gamma\,\Delta H \tag{5}$$

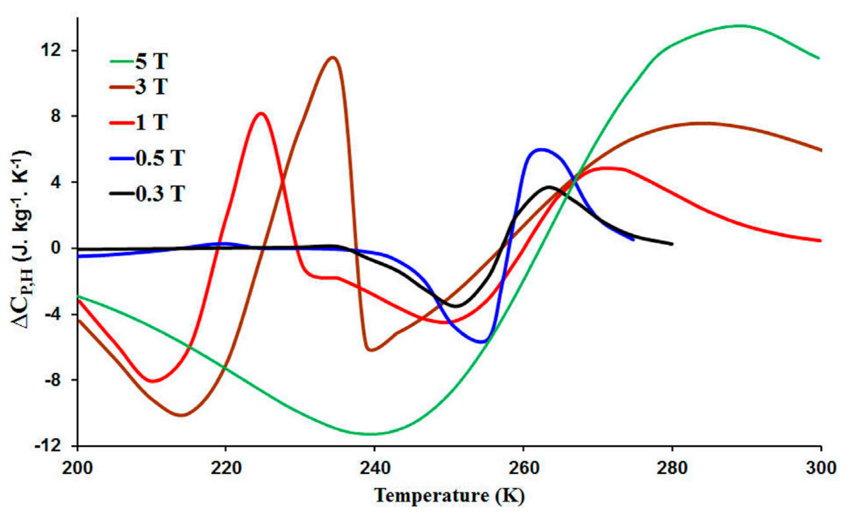

FIGURE 4 | $\Delta C_{P,H}$ *vs.* temperature for $La_{0.5}Ca_{0.1}Ag_{0.4}MnO_3$.

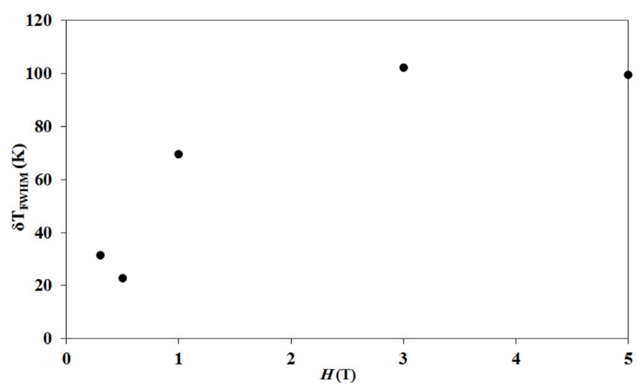

FIGURE 6 | δT_{FWHM} *vs.* ΔH for $La_{0.5}Ca_{0.1}Ag_{0.4}MnO_3$.

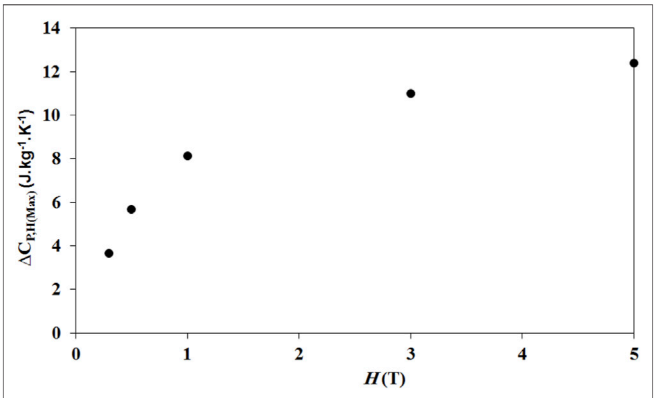

FIGURE 8 | $\Delta C_{P,H(max)}$ *vs.* ΔH for $La_{0.5}Ca_{0.1}Ag_{0.4}MnO_3$.

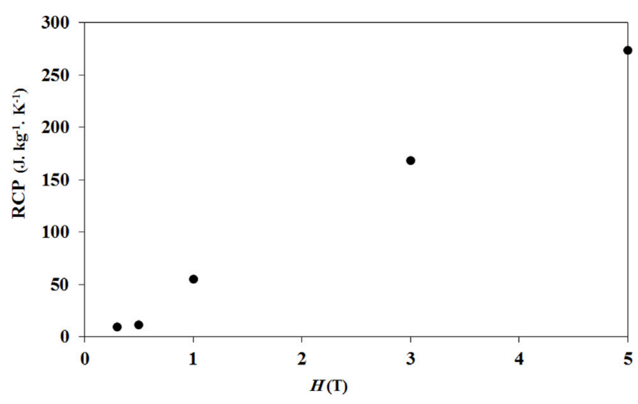

FIGURE 7 | Relative cooling power *vs.* ΔH for $La_{0.5}Ca_{0.1}Ag_{0.4}MnO_3$.

The full-width at half-maximum (δT_{FWHM}) of LCAMO can be given as follows:

$$\delta T_{FWHM} = \frac{2}{\alpha}\cosh^{-1}\left(\left|\sqrt{\frac{2\alpha\left(M_i - M_f\right)}{\alpha\left(M_i - M_f\right) + 2\beta}}\right|\right) \tag{6}$$

A magnetic cooling efficiency of LCAMO is expected by considering the magnitude of $|\Delta S_{Max}(T, H_{max})|$ and δT_{FWHM} (Hamad, 2012). RCP is calculated as follows:

$$RCP = \delta T_{FWHM} \times |\Delta S_{Max}(T, H_{max})| \tag{7}$$

The $\Delta C_{P,H}$ of LCAMO can be given as follows (Hamad, 2012):

$$\Delta C_{P,H} = -\Delta H \alpha^2 T\left(M_i - M_f\right)\tanh\left(\alpha\left(\theta_c - T\right)\right)\mathrm{sech}^2\left(\alpha\left(\theta_c - T\right)\right). \tag{8}$$

RESULTS AND DISCUSSION

At values of H_{ext} <5 T, there are two magnetic transitions of LCAMO, as can be observed in **Figure 2**, at two different temperatufvariation, which is about 57% of the correspondingres. It is possible that this is due to the presence of a canted FM phase in the FM matrix, which can be attributed to the additional Ag content (Jeddi et al., 2020), thus expecting two peaks in the ΔS_M curves. However, at H_{ext} = 5 T, it seems like a single magnetic transition of LCAMO, expecting a single peak in the ΔS_M curve. It is possible that this is due to the presence of a strong interatomic double exchange interaction at H_{ext} = 5 T. To simulate the MCE of LCAMO, the PM parameters (M_i, M_f, Θ_c, β, and α) of LCAMO for each magnetic transition were determined directly from experimental data (isofield magnetization *vs.* temperature) as in Jeddi *et al.* (2020). We can see from **Figure 2** that there is a good agreement between the experimental and theoretical results of $M(T)$, confirming the good fit of this model for simulating the MCE of LCAMO. This work demonstrates the good coincidence between the experimental data and the continuous curves given by PM, indicating that this model allows us to predict the MCE for LCAMO under different magnetic fields. The $M(T)$ curves of LCAMO demonstrate the magnetic transition from the FM phase to a paramagnetic one under different magnetic fields. The θ_C increases as H_{ext} increases due to the increased alignment of the local spins, resulting in an increase in the interatomic double exchange interaction. As shown in **Figure 3A**, there are two peaks in the $\Delta S_M(T)$ curves when H_{ext} <5 T. However, at H_{ext} = 5 T, there is a single peak in the ΔS_M curve due to the large interatomic double exchange. ΔS_M reaches a peak of 2.75 J/kg K. Though the maximum ΔS_M is 2.75 J/kg K upon 5T applied field variation, which is about 57% of the corresponding value of the compound that belongs to the same system as $La_{0.5}Ca_{0.2}Ag_{0.3}MnO_3$ (ΔS_{Max} = 4.8 J/kg K upon 5 T), the value of RCP (273.5 J/kg upon 5 T) is larger, and the ΔS_M distribution of LCAMO is much more broad than that of $La_{0.5}Ca_{0.2}Ag_{0.3}MnO_3$ (RCP = 168 J/kg δT_{FWHM} = 35 upon 5 T), covering a wider range of temperature (Felhi et al., 2019). **Figure 3B** shows that $\Delta S_M(T)$ was calculated by Maxwell relation from experimental isothermal magnetization as a function of H in Ref. 31, and $\Delta S_M(T)$ was calculated by PM, ranging between 240 and 270 K and covering the highest temperature transition. There is a good agreement and approach between the calculated results of both Maxwell relation and PM. Therefore, these results confirm that **Eq. 4** still holds at ΔH of 0.5, 1, 3, and 5 T.

TABLE 1 | The comparison of magnetocaloric effect parameters for $La_{0.5}Ca_{0.1}Ag_{0.4}MnO_3$ (LCAMO) with corresponding ones of various magnetocaloric effect materials in high ΔH.

Compounds	θ_C (K)	ΔH (T)	$\|\Delta S_{Max}\|$ (J/kg K)	Relative cooling power (J/kg)	Reference
LCAMO	282	5	2.75	273.5	This work
$Fe_{68.8}Cr_{11.2}Si_6B_{14}$	300	5	1.8	340.2	Álvarez-Alonso *et al.* (2013)
$Yb_{0.9}Er_{0.1}MnO_3$	3.7	8	2	23.1	Bhumireddi *et al.* (2015)
$Yb_{0.8}Er_{0.2}MnO_3$	3.7	8	2.1	23.8	Bhumireddi *et al.* (2015)
$Fe_{68}Cr_{12}Si_8B_{12}$	360	5	2.1	310	El Boubekri *et al.* (2020)
$La_{0.5}Ca_{0.5}Mn_{0.9}V_{0.1}O_3$	263	5	2.42	162.8	Mansouri *et al.* (2016)
SmCrO3	190	5	0.11	1.7	Gupta and Poddar, (2016)
$La_{1.1}Bi_{0.3}Sr_{1.6}Mn_2O_7$	340	5	1.65	134.4	Oubla *et al.* (2016)
$La_{0.45}Bi_{0.15}Sr_{0.4}CoO_3$	190	5	1.24	106.6	Saadaoui *et al.* (2013)
$La_{0.6}Sr_{0.4}CoO_3$	230	5	2.28	143.6	Saadaoui *et al.* (2013)
$Pr_{0.5}K_{0.05}Sr_{0.45}MnO_3$	310	5	1.66	272.5	Jerbi *et al.* (2015)
$Pr_{0.5}Na_{0.05}Sr_{0.45}MnO_3$	270	5	1.60	266.2	Jerbi *et al.* (2015)
$Ce_{0.67}Sr_{0.33}MnO_3$	48	5	1.65	41.41	Hamad (2013)
$Fe_{60}Ru_{20}B_{20}$	255	5	1.52	394	Boutahar *et al.* (2015)
$LaCrO_3$	288	9	0.11	1.1	Biswal *et al.* (2019)
$Pr_{0.5}Sr_{0.5}CoO_3$	218	5	2.2	84	Ho *et al.* (2014)
$Pr_{0.6}Sr_{0.4}CoO_3$	204	5	1.9	52	Ho *et al.* (2014)
$La_{0.5}Sr_{0.5}CoO_3$	253	5	2.49	141.2	Long *et al.* (2018)

Figure 4 shows that $\Delta C_{P,H}(T)$ has an inverse change from a negative change to a positive one at around θ_C for each magnetic transition, causing a modification in the total specific heat. This oscillating temperature dependence of $\Delta C_{P,H}(T)$ at different temperatures is a reflection of $\Delta S_M(T)$ behavior. The behavior of $|\Delta S_M|$ and $\Delta C_{P,H}(T)$ curves suggests how the range of temperature for functioning LCAMO in the MR can be expanded. It is clear that the $|\Delta S_M|$ and $\Delta C_{P,H}$ peaks of LCAMO extend over a large temperature range. This temperature range of $|\Delta S_M|$ and $\Delta C_{P,H}$ expanded with increasing variation in H_{ext}, *i.e.*, the peaks broaden, covering room temperature upon high values of ΔH. This indicates that larger $|\Delta S_M|$ and ΔCP, H are expected at higher values of ΔH. Moreover, the variation of H_{ext} allows the tuning of θ_C of LCAMO. This tunable θ_C makes LCAMO practically more helpful for the development of MRs.

Figures 5–8 show the values of $|\Delta S_{Max}|$, δT_{FWHM}, RCP, and $\Delta C_{P,H(Max)}$ (maximum value of $\Delta C_{P,H}$) for LCAMO, respectively. It is clear that $|\Delta S_{Max}|$, RCP, and $\Delta C_{P,H(max)}$ show a general increase with an increase in ΔH due to enhancing the variations of alignment in the local spins with an increase in ΔH, resulting in an increase in MC properties.

These large values of $|\Delta S_{Max}|$, δT_{FWHM}, RCP, and $\Delta C_{P,H(Max)}$ in LCAMO prevailed as well in perovskite manganite due to the strong coupling between spin and lattice (Dhahri et al., 2008). Since lattice change is associated to magnetic transition in the manganite, this caused a further change in the magnetism of manganite (Dhahri et al., 2008). Furthermore, the bond distance of <Mn–O> plus bond angle <Mn–O–Mn> changes to favor the spin ordering with a high value of H_{ext}, leading to enhanced $|\Delta S_{Max}|$, δT_{FWHM}, RCP, and $\Delta C_{P,H(Max)}$ in LCAMO (Radaelli et al., 1995; Hamad, 2015b).

Table 1 gives a comparative importance of the MCE parameters of LCAMO with those of various materials in terms of the high values of ΔH in previous works (Álvarez-Alonso et al., 2013; Hamad, 2013; Saadaoui et al., 2013; Ho et al., 2014; Bhumireddi et al., 2015; Boutahar et al., 2015; Jerbi et al., 2015; Gupta and Poddar, 2016; Mansouri et al., 2016; Oubla et al., 2016; Long et al., 2018; Biswal et al., 2019; El Boubekri et al., 2020). The MCE parameters of LCAMO are significantly larger than some MCE parameters of MC samples in the corresponding values of ΔH and the higher ones. From this comparative image, we conclude that LCAMO can function as a favorable MC magnet for the MR.

CONCLUSION

Based on thermodynamic calculation *via* PM, the MCE of LCAMO is simulated under different values of variation in H_{ext}. The MCE of LCAMO is strongly tunable with the value of the variation of H_{ext}. Therefore, LCAMO can be used over a wide temperature range as an effective material for MR, covering a large range of temperatures, including room temperature and lower and higher ones. The MCE of LCAMO is tunable with the variation of H_{ext}, proving that LCAMO is practically more helpful as a MC magnet for the development of MRs in an extensive temperature range, including room temperature. The values of the MCE parameters of LCAMO are practically greater than the MCE ones of some MC samples in earlier works.

DATA AVAILABILITY STATEMENT

The original contributions presented in the study are included in the article/supplementary material. Further inquiries can be directed to the corresponding author.

AUTHOR CONTRIBUTIONS

All authors listed have made a substantial, direct, and intellectual contribution to the work and approved it for publication.

REFERENCES

Ahmed, E. M., Alamri, H. R., Elghnam, S. M., Eldarawi, O., Tawfik, T. E., Mahmoud, A. M., et al. (2021). Tuning Magnetocaloric Properties for La1 -xSrxCoO3. *Phys. Solid State.* doi:10.1134/S1063783421100024

Ahmed, E. M., Hemeda, O. M., Alamri, H. R., Elghnam, S. M., and Hamad, M. A. (2021). Investigation of Thermomagnetic Properties in Ca3Co2O6 over Cryogenic Temperature between 0 and 100 K. *Phase Transitions.* 94, 835–841. doi:10.1080/01411594.2021.1975706

Álvarez-Alonso, P., Santos, J. D., Pérez, M. J., Sánchez-Valdes, C. F., Sánchez, J. L., and Gorria, P. (2013). The Substitution Effect of Chromium on the Magnetic Properties of (Fe1− xCrx) 80Si6B14 Metallic Glasses (0.02≤ X≤ 0.14). *J.Magn.Magn.Mater.* 347, 75–78.

Alzahrani, B., Hsini, M., Hcini, S., Boudard, M., Dhahri, A., and Bouazizi, M. L. (2020). Study of the Magnetocaloric Effect by Means of Theoretical Models in La0.6Ca0.2Na0.2MnO3 Manganite Compound. *J. Low Temp Phys.* 200, 26–39. doi:10.1007/s10909-020-02455-w

Belhamra, S., Masrour, R., Jabar, A., and Hlil, E. K. (2021). A Comparative Study of the Structural, Electronic, Magnetic Properties and Magnetocaloric Effect of Perovskite LaRO3 (R = Mn, Cr and Fe). *Polyhedron.* 193, 114891. doi:10.1016/j.poly.2020.114891

Bhumireddi, S., Bhatnagar, A. K., Singh, D., Rayaprol, S., Das, D., and Ganesan, V. (2015). Specific Heat and Magnetocaloric Studies of Hexagonal Yb1−xErxMnO3. *Mater. Lett.* 161, 419–422. doi:10.1016/j.matlet.2015.08.151

Biswal, H., Singh, V., Nath, R., Angappane, S., and Sahu, J. R. (2019). Magnetic and Magnetocaloric Properties of LaCr1-xMnxO3 (X = 0, 0.05, 0.1). *Ceramics Int.* 45, 22731–22736. doi:10.1016/j.ceramint.2019.07.311

Boutahar, A., Lassri, H., and Hlil, E. K. (2015). Magnetic, Magnetocaloric Properties and Phenomenological Model in Amorphous Fe60Ru20B20 Alloy. *Solid State. Commun.* 221, 9–13. doi:10.1016/j.ssc.2015.08.002

Choura-Maatar, S., Nofal, M. M., M'nassri, R., Cheikhrouhou-Koubaa, W., Chniba-Boudjada, N., and Cheikhrouhou, A. (2020). Enhancement of the Magnetic and Magnetocaloric Properties by Na Substitution for Ca of La0.8Ca0.2MnO3 Manganite Prepared via the Pechini-type Sol-Gel Process. *J. Mater. Sci. Mater. Electron.* 31, 1634–1645. doi:10.1007/s10854-019-02680-4

Dhahri, A., Dhahri, E., and Hlil, E. K. (2014). Structural Characterization, Magnetic Properties and Magnetocaloric Effects of La0.75Sr0.25Mn1-X Cr X O3 (X = 0.15, 0.20, and 0.25). *Appl. Phys. A.* 116, 2077–2085. doi:10.1007/s00339-014-8404-5

Dhahri, A., Jemmali, M., Dhahri, E., and Valente, M. A. (2015). Structural Characterization, Magnetic, Magnetocaloric Properties and Phenomenological Model in Manganite La0.75 Sr0.1Ca0.15 MnO3 Compound. *J. Alloys Compounds.* 638, 221–227. doi:10.1016/j.jallcom.2015.01.314

Dhahri, J., Dhahri, A., Oumezzine, M., and Dhahri, E. (2008). Effect of Sn-Doping on the Structural, Magnetic and Magnetocaloric Properties of La0.67Ba0.33Mn1−xSnxO3 Compounds. *J. Magnetism Magn. Mater.* 320, 2613–2617. þ. doi:10.1016/j.jmmm.2008.05.030

El Boubekri, A., Tillaoui, S., Sajieddine, M., Sahlaoui, M., Lassri, H., Hlil, E. K., et al. (2020). Magnetic and Magnetocaloric Properties of Fe68+Cr12−Si8B12 Ribbons. *J. Magnetism Magn. Mater.* 507, 166819. doi:10.1016/j.jmmm.2020.166819

El-Sayed, A. H., and Hamad, M. A. (2019a). Nickle Concentration Effect on Low Magnetic Field Magnetocaloric Properties for Ni2+xMn1−xGe. *J. Supercond. Nov. Magn.* 32, 1447–1450. doi:10.1007/s10948-018-4855-9

El-Sayed, A. H., and Hamad, M. A. (2019b). Tailoring Thermomagnetic Properties in Pb(Zr0.52Ti0.48)O3-Ni(1−x)ZnxFe2O4. *Phase Transitions.* 92, 517–524. doi:10.1080/01411594.2019.1597096

ErchidiElyacoubi, A. S., Masrour, R., and Jabar, A. (2018a). Surface Effects on the Magnetocaloric Properties of Perovskites Ferromagnetic Thin Films: A Monte Carlo Study. *Appl. Surf. Sci.* 459, 537–543. þ. doi:10.1016/j.apsusc.2018.08.020

ErchidiElyacoubi, A. S., Masrour, R., and Jabar, A. (2018b). Magnetocaloric Effect and Magnetic Properties in SmFe1-xMnxO3 Perovskite: Monte Carlo Simulations. *Solid State. Commun.* 271, 39–43. þ. doi:10.1016/j.ssc.2017.12.015

Erchidi Elyacoubi, A. S., Masrour, R., Jabar, A., Ellouze, M., and Hlil, E. K. (2018c). Magnetic Properties and Magnetocaloric Effect in Double Sr2FeMoO6 Perovskites. *Mater. Res. Bull.* 99, 132–135. doi:10.1016/j.materresbull.2017.10.037

Felhi, H., Dhahri, R., Smari, M., Dhahri, E., and Hlil, E. K. (2019). Magnetocaloric Effect and Critical Behaviour of La0.5Ca0.2Ag0.3MnO3 Compound. *Chem. Phys. Lett.* 733, 136632. doi:10.1016/j.cplett.2019.136632

Gupta, P., and Poddar, P. (2016). Study of Magnetic and thermal Properties of SmCrO3 Polycrystallites. *RSC Adv.* 6, 82014–82023. doi:10.1039/c6ra17203b

Hamad, M. A. (2012). Prediction of Thermomagnetic Properties of La0.67Ca0.33MnO3and La0.67Sr0.33MnO3. *Phase Transitions* 85, 106–112. doi:10.1080/01411594.2011.605027

Hamad, M. A. (2013). Magnetocaloric Effect of Perovskite Manganites Ce0.67Sr0.33MnO3. *J. Supercond Nov Magn.* 26, 2981–2984. doi:10.1007/s10948-013-2124-5

Hamad, M. A. (2015a). Lanthanum Concentration Effect of Magnetocaloric Properties in La_x $MnO_{3-\delta}$. *J. Supercond Nov Magn.* 28, 173. doi:10.1007/s10948-014-2834-3

Hamad, M. A. (2015b). Magnetocaloric Effect in Sr2FeMoO6/Ag Composites. *Process. Appl. Ceram.* 9, 11. doi:10.2298/PAC1501011H

Hamad, M. A. (2015c). Effects of Addition of Rare Earth on Magnetocaloric Effect in Fe82Nb2 B 14. *J. Supercond. Nov. Magn.* 28, 3111–3115. doi:10.1007/s10948-015-3140-4

Hamad, M. A. (2015d). Magnetocaloric Effect in La1-X Ce X MnO3. *J. Adv. Ceram.* 4, 206–210. doi:10.1007/s40145-015-0150-4

Hamad, M. A., Hemeda, O. M., and Mohamed, A. M. (2020). Investigations on Enhancing Thermomagnetic Properties in $Co_xZn_{1-x}Fe_2O_4$. *J. Supercond. Nov. Magn.* 33, 2753–2757. doi:10.1007/s10948-020-05503-4

Hamad, M. A., Hemeda, O. M., Alamri, H. R., and Mohamed, A. M. (2021). Investigations on Thermomagnetic Properties of YbFe2As2. *J. Low Temp Phys.* 202, 121–127. þ. doi:10.1007/s10909-020-02528-w

Henchiri, C., Mnasri, T., Benali, A., Hamdi, R., Dhahri, E., Valente, M. A., et al. (2020). Structural Study and Large Magnetocaloric Entropy Change at Room Temperature of La1−x□xMnO3 Compounds. *RSC Adv.* 10, 8352–8363. þdoi:10.1039/c9ra10469k

Ho, T. A., Thanh, T. D., Ho, T. O., Tran, Q. T., Phan, T. L., and Yu, S. C. (2014). Critical Behavior and Magnetocaloric Effect of $Pr_{1-x}Sr_xCoO_3$. *IEEE Trans. Magn.* 50, 2505104. doi:10.1109/tmag.2014.2322906

Jebari, H., Tahiri, N., Boujnah, M., El Bounagui, O., Taibi, M., and Ez-Zahraouy, H. (2021). Theoretical Investigation of Electronic, Magnetic and Magnetocaloric Properties of Bi25FeO40 Compound. *Phase Transitions.* 94, 147–158. doi:10.1080/01411594.2021.1931690

Jeddi, M., Gharsallah, H., Bekri, M., Dhahri, E., and Hlil, E. K. (2020). Phenomenological Modeling of Magnetocaloric Properties in 0.75La0.6Ca0.4MnO3/0.25La0.6Sr0.4MnO3 Nanocomposite Manganite. *J. Low Temp Phys.* 198, 135–144. doi:10.1007/s10909-019-02256-w

Jerbi, A., Krichene, A., Chniba-Boudjada, N., and Boujelben, W. (2015). Magnetic and Magnetocaloric Study of Manganite Compounds Pr0.5A0.05Sr0.45MnO3 (A=Na and K) and Composite. *Physica B: Condensed Matter* 477, 75–82. doi:10.1016/j.physb.2015.08.022

Kadim, G., Masrour, R., and Jabar, A. (2020). Large Magnetocaloric Effect, Magnetic and Electronic Properties in Ho3Pd2 Compound: Ab Initio Calculations and Monte Carlo Simulations. *J. Magnetism Magn. Mater.* 499, 166263. þ. doi:10.1016/j.jmmm.2019.166263

Kadim, G., Masrour, R., Jabar, A., and Hlil, E. K. (2021a). Room-Temperature Large Magnetocaloric, Electronic and Magnetic Properties in La0.75Sr0.25MnO3 Manganite: Ab Initio Calculations and Monte Carlo Simulations. *Physica A: Stat. Mech. its Appl.* 573þ, 125936. doi:10.1016/j.physa.2021.125936

Kadim, G., Masrour, R., and Jabar, A. (2021b). Magnetocaloric Effect, Electronic and Magnetic Properties of Ba1-xSrxFeO3 Barium-Strontium Ferrites: Monte Carlo Simulations and Comparative Study between TB-mBJ and GGA+U. *Mater. Today Commun.* 26, 102071. doi:10.1016/j.mtcomm.2021.102071

Laajimi, K., Khlifi, M., Hlil, E. K., Gazzah, M. H., Ayed, M. B., Belmabrouk, H., et al. (2020). Influence of Sr Substitution on Structural, Magnetic and Magnetocaloric Properties in La0.67Ca0.33−xSrxMn0.98Ni0.02O3 Manganites. *J. Mater. Sci. Mater. Electron.* 31, 15322–15335. þ. doi:10.1007/s10854-020-04096-x

Labidi, S., Masrour, R., Jabar, A., and Ellouze, M. (2021). Mechanical, Electronic and Magnetic Properties of Double Sr2FeMoO6 Perovskite: Density Functional

Theory and Monte Carlo Simulation. *J. Magnetism Magn. Mater.* 523, 167594. þ. doi:10.1016/j.jmmm.2020.167594

Long, P. T., Manh, T. V., Ho, T. A., Dongquoc, V., Zhang, P., and Yu, S. C. (2018). Magnetocaloric Effect in La1-xSrxCoO3 Undergoing a Second-Order Phase Transition. *Ceramics Int.* 44, 15542–15549. doi:10.1016/j.ceramint.2018.05.216

Mansouri, M., Omrani, H., Cheikhrouhou-Koubaa, W., Koubaa, M., Madouri, A., and Cheikhrouhou, A. (2016). Effect of Vanadium Doping on Structural, Magnetic and Magnetocaloric Properties of La 0.5 Ca 0.5 MnO 3. *J. Magnetism Magn. Mater.* 401, 593–599. doi:10.1016/j.jmmm.2015.10.066

Masrour, R., Jabar, A., Benyoussef, A., Hamedoun, M., and Hlil, E. K. (2016). Monte Carlo Simulation Study of Magnetocaloric Effect in NdMnO 3 Perovskite. *J. Magnetism Magn. Mater.* 401, 91–95. þ. doi:10.1016/j.jmmm.2015.10.019

Masrour, R., Jabar, A., Khlif, H., Jemaa, F. B., Ellouze, M., and Hlil, E. K. (2017). Experiment, Mean Field Theory and Monte Carlo Simulations of the Magnetocaloric Effect in La 0.67 Ba 0.22 Sr 0.11 MnO 3 Compound. *Solid State. Commun.* 268, 64–69. þ. doi:10.1016/j.ssc.2017.10.003

Oubla, M., Lamire, M., Boutahar, A., Lassri, H., Manoun, B., and Hlil, E. K. (2016). Structural, Magnetic and Magnetocaloric Properties of Layered Perovskite La1.1Bi0.3Sr1.6Mn2O7. *J. Magnetism Magn. Mater.* 403, 114–117. doi:10.1016/j.jmmm.2015.11.076

Radaelli, P. G., Cox, D. E., Marezio, M., Cheong, S.-W., Schiffer, P. E., and Ramirez, A. P. (1995). Simultaneous Structural, Magnetic, and Electronic Transitions inLa1−xCaxMnO3withx=0.25 and 0.50. *Phys. Rev. Lett.* 75, 4488–4491. doi:10.1103/physrevlett.75.4488

Saadaoui, F., Koubaa, M., Cheikhrouhou-Koubaa, W., and Cheikhrouhou, A. (2013). Effects of Bismuth Doping on the Physical Properties of La0.6−x Bi X Sr0.4CoO3 (0≤x≤0.15) Cobaltites. *J. Supercond. Nov. Magn.* 26, 3043–3047. doi:10.1007/s10948-013-2122-7

Sharma, P., Masrour, R., Jabar, A., Fan, J., Kumar, A., Ling, L., et al. (2020). Structural and Magnetocaloric Properties of Rare-Earth Orthoferrite Perovskite: TmFeO3. *Chem. Phys. Lett.* 740, 137057. þ. doi:10.1016/j.cplett.2019.137057

Conflict of Interest: The authors declare that the research was conducted in the absence of any commercial or financial relationships that could be construed as a potential conflict of interest.

Publisher's Note: All claims expressed in this article are solely those of the authors and do not necessarily represent those of their affiliated organizations or those of the publisher, the editors, and the reviewers. Any product that may be evaluated in this article or claim that may be made by its manufacturer is not guaranteed or endorsed by the publisher.